An adaptive, real-time cadence algorithm for unconstrained sensor placement

van Oeveren, B. T.; de Ruiter, C. J.; Beek, P. J.; Rispens, S. M.; van Dieën, J. H.

published in
Medical Engineering and Physics
2018

DOI (link to publisher)
10.1016/j.medengphy.2017.12.007

document version
Publisher's PDF, also known as Version of record

Medical Engineering and Physics 52 (2018) 49–58

Contents lists available at ScienceDirect

Medical Engineering and Physics

journal homepage: www.elsevier.com/locate/medengphy

An adaptive, real-time cadence algorithm for unconstrained sensor placement

B.T. van Oeveren*, C.J. de Ruiter*, P.J. Beek, S.M. Rispens, J.H. van Dieën

Department of Human Movement Sciences, Faculty of Behavioural and Movement Sciences, Vrije Universiteit Amsterdam, Amsterdam Movement Sciences, The Netherlands

ARTICLE INFO

Article history:
Received 24 March 2017
Revised 15 December 2017
Accepted 22 December 2017

Keywords:
Running
Gait cycle detection
Stride frequency
Accelerometer
Cadence
Sylvester's criterion
Cross-correlation
Autocorrelation

ABSTRACT

This paper evaluates a new and adaptive real-time cadence detection algorithm (CDA) for unconstrained sensor placement during walking and running. Conventional correlation procedures, dependent on sensor position and orientation, may alternately detect either steps or strides and consequently suffer from false negatives or positives. To overcome this limitation, the CDA validates correlation peaks as strides using the Sylvester's criterion (SC). This paper compares the CDA with conventional correlation methods.

22 volunteers completed 7 different circuits (approx. 140 m) at three gaits-speeds: walking (1.5 m s^{-1}), running (3.4 m s^{-1}), and sprinting (5.2 and 5.7 m s^{-1}), disturbed by various gait-related activities. The algorithm was simultaneously evaluated for 10 different sensor positions. Reference strides were obtained from a foot sensor using a dedicated offline algorithm.

The described algorithm resulted in consistent numbers of true positives (85.6–100.0%) and false positives (0.0–2.9%) and showed to be consistently accurate for cadence feedback across all circuits, subjects and sensors (mean ± SD: 98.9 ± 0.2%), compared to conventional cross-correlation (87.3 ± 13.5%), biased (73.0 ± 16.2) and unbiased (82.2 ± 20.6) autocorrelation procedures.

This study shows that the SC significantly improves cadence detection, resulting in robust results for various gaits, subjects and sensor positions.

1. Introduction

All forms of human locomotion are cyclic in nature. Understandably, the detection of the fundamental movement frequency (cadence) is of interest and has served as a basis for physical activity assessment [1,2], activity recognition [3,4] and detection of spatiotemporal events within the gait cycle (e.g. initial contact, toe-off) [5–8]. In addition, cadence is related to energy expenditure in running [12], swimming [9], skating [10] and rowing [11] and impact forces [13] in running. The use of electronic devices, such as sport watches and smartphones, is rapidly increasing [14]. These devices are commonly equipped with tri-axial accelerometers used to provide feedback on cadence. However, the devices are carried at many different locations on the body, while sensor orientation and position may have a large impact on the accuracy of cadence detection. Especially the smartphone is often loosely fixated and carried with variable orientation. Cadence detection is further challenged by gait transitions and variation between activities, such as walking, running and climbing stairs and by gait-related interruptions, such as stopping, going through a fence, or stepping over an obstacle. Lastly, the algorithms are expected to provide real-time feedback and consequently computation on the device is required. Clearly, the diverse usage of devices in everyday conditions challenges algorithms for accurate cadence detection.

Different approaches to estimate cadence have been proposed. Approaches can be divided in clustering, time-domain and frequency-domain techniques [15]. Each approach has specific advantages and disadvantages. The clustering techniques require training of a model, which makes generalization and quick adaptation across various situations and sensor orientations difficult. In the time-domain, acceleration signals are typically first low-pass filtered before detection of peak or zero-crossings [15,16]. The disadvantage is that variations in sensor position, sensor fixation, terrain and activity require dynamic thresholds for peak detection. Sensor position and movement intensity alter the signal-to-noise ratio, which makes peak detection in the time-domain prone to false positives or negatives [17].

Alternatively, the cadence can be estimated in the frequency domain using the Fast Fourier Transformation (FFT) [6,17–19]. Disadvantage of the FFT are resolution problems that occur

* Corresponding authors at: Department of Human Movement Sciences, Vrije Universiteit Amsterdam, Van der Boechorststraat 9, 1081 BT Amsterdam, The Netherlands.

E-mail addresses: b.t.van.oeveren@vu.nl (B.T. van Oeveren), c.j.de.ruiter@vu.nl (C.J. de Ruiter).

https://doi.org/10.1016/j.medengphy.2017.12.007
1350-4533/

depending on the choice of the (time) window length [15]. With long windows, the accuracy of the frequency estimate is reduced and feedback will be delayed [17]. On the other hand, short windows reduce the relative power at the dominant frequency and consequently the reliability of the estimate. Wavelet analysis has been introduced as an alternative [21]. However, the optimization process underlying the wavelet analysis makes the computational load relatively high [21] and therefore wavelet analysis is considered to be less useful for real-time analysis and on-sensor processing.

Correlation procedures share advantages and disadvantages with frequency domain techniques, but the correlation spectrum corresponds directly with the time-domain (Figs. 2 and 3). In walking and running, peak correlation coefficients are found when the original signal and its time-delayed copy (autocorrelation) have an overlap of one step or stride, depending on the sensor position and orientation. The correlation peaks represent the average periodicity over the chosen window. Crucial steps in correlation procedures are the choice of the window length, selection of the signal and the procedure to detect the peak that represents the true fundamental movement frequency. As an alternative to autocorrelation, cross-correlation procedures are used for template matching [16,20], where an online or offline defined template is correlated to the signal. A disadvantage of template-matching is that the template has to resemble the signal quite closely for accurate detection and therefore is prone to suffer from mismatches. Cross-correlation procedures [15,22,23] can also be applied without a pre-defined template, which may improve generalizability and adaptiveness. Cross-correlation procedures without pre-defined templates compare sequential movement traces.

When the orientation of the sensor is known, the vertical acceleration is often isolated [17,24] and used for the correlation procedure. Note that changes in sensor orientation during the activity may reduce accuracy. When the orientation is unknown, two solutions are often applied:

(i) The orientation of the sensor's local axes is re-aligned to match the global (earth) orientation. To this end, gyroscopes (and magnetometers) are often used. Note that the re-alignment should be representative throughout the movement. For real-time processing, the processing of multiple sensors simultaneously is disadvantageous for the computational load and battery life [15].

(ii) Alternatively, the magnitude of the acceleration signal is calculated [17,24]. Note that by calculating the magnitude, directional information is lost. Consequently, the signal frequency increases, which may increase the number of false positives. Without differentiation between half cycles (steps) versus whole cycles (strides) the algorithm is dependent on the sensor position. Centrally placed sensors will tend to detect steps, while sensors placed on the limbs will tend to detect strides. The sensors placed outside the midline but central on the body, such as sensors placed round the hip, will likely result in inaccurate cadence detection since they will inconsequently detect steps or strides. Moreover, when the goal is to detect steps, asymmetrical gait patterns, orientation, fixation and mediolateral placement will likely cause differences in left and right acceleration patterns. Such situations occur frequently in everyday conditions and may reduce the power of correlation between sequential steps. We reasoned that the correlation between two sequential strides may provide more stable cadence estimation and prevent step-stride confusions by verifying correlation peaks using the Sylvester's criterion (SC). The SC requires all directions of the reference signal to correlate positively with all directions of the incoming signal, this prevents the need to isolate a certain axis or to combine axes and makes the algorithm independent of sensor orientation.

Previous studies have described algorithms with reasonable to good results for the estimation of movement frequencies. These algorithms were often specifically designed for walking (e.g. [4,6,17,24]). Moreover, as argued by others, validation protocols have been often overly simplified and did not represent the variability of everyday conditions [2,15,17]. Furthermore, many algorithms rely on specific constraints, often sensor position and orientation have to be known and/or multiple sensors have to be used [4,6]. To our knowledge, there is no algorithm yet capable of dealing simultaneously with (i) unconstrained sensor placement; (ii) everyday conditions and (iii) real-time processing on the sensor. Therefore, the goal of the current study was to design and validate an algorithm that accurately detects strides and provides cadence feedback during walking and running under unconstrained conditions.

2. Material and methods

2.1. Subjects

Twenty-two healthy subjects (nine females, thirteen males, 28 ± 2.9 yrs, 178 ± 9.5 cm and 70 ± 10 kg) participated in this study. Subjects were recruited from the university population. All subjects provided written consent approved by the local ethics committee of the Vrije Universiteit Amsterdam in accordance with the guidelines set out in the Helsinki Declaration regarding human research.

2.2. Equipment

Accelerometer data were gathered from 3 Samsung Galaxy S4 phones (136.6 × 69.8 × 7.9 mm, 130 g (weight), 100 Hz, $\pm 19.6\,g$ (range)) and 7 small 9-DOF IMU's (MPU-9150, Invensense, San Jose, USA: 35 × 25 × 11 mm, ±12.5 g (weight), 500 Hz, $\pm 16.0\,g$ (range)). Sensor fixation differed per position, the sensors on the leg were strapped with elastic bands, shoe-sensors were taped, one phone was worn in the trouser pocket, the phones carried on the upper arm and around the waist (on the back) were placed in commercial neoprene belts and a dummy phone with a sensor was held in the hand. To measure speed, a GPS watch (Garmin Forerunner 620) was used. Activities were labelled afterwards using video footage (60 Hz) of three cameras. To enable actual implementation on the smartphone, the algorithm was simultaneously optimized for Java code and tested on Samsung Galaxy S4 phones. However, this paper focusses on the method and analysis performed offline in Matlab.

2.3. Protocol

Subjects had to walk or run outdoors back and forth on seven different circuits (distances of about 140 m, 210 m and 50 m) at three freely chosen gait speeds: walking, running, sprinting. Sprinting was performed under two conditions: with a sudden start and stop and with gradual acceleration and deceleration. Within each circuit, the regularity of the movement was interrupted by short gait-related activities, such as turns, jumping, slalom, speed ladder, answering the phone and stair walking. To further challenge the algorithm, most circuits were performed twice, once on paved and once on a grass surface (Table 1). Participants were free to fixate the 10 sensors in a way they felt comfortable for running. The researcher only assisted with the placement of these sensors. Prior to the measurements, participants were informed about the type of activity, without detailed instructions on the execution of the activity. The IMU's started sampling simultaneously once they were removed from their power source. To synchronize the smartphones with the IMUs and video footage, the participants were asked to make a jump prior to the actual experiment, which caused a clear peak in the acceleration signal that was used for synchronization.

Table 1
Circuits. The subjects completed 7 different circuits interrupted by various gait-related activities performed on two types of surfaces. The length of the long jump was freely chosen. For the speed ladder and the slalom 6 lines, 60 cm apart in running direction where taped to the ground. Line 1, 3, 5 had 60 cm overlap with line 2, 4, 6 in sideward direction. In the speed ladder condition, subjects had to place their feet between the lines. During the slalom, the subjects had to slalom between the lines. The stair consisted of 11 steps. During answering the phone condition, the phone was picked up from the trouser pocket and held against the ear for approximately 10 m during walking.

Circuit	Activity							Surface	
								First time	Second time
1		Run (70 m)		Turn_1	Run (20 m)	Walk (30 m)	Run (20 m)	Paved	
2	Run (20 m)	Jump (±2 m)	Run (48 m)	Turn_1	Run (47 m)	Slalom (3 m)	Run (20 m)	Paved	Grass
3	Run (20 m)	Speed ladder (3 m)	Run (47 m)	Turn_1	Run (47 m)	Speed ladder (3 m)	Run (20 m)	Grass	Paved
4		Sprint 1 (70 m)		Turn_1	Walk (30 m)	Answer phone (10 m)	Run (20 m)	Grass	
5		Sprint 2 (105 m)		Turn_2	Run (65 m)	Answer phone (10 m)	Walk (20 m)	Paved	Grass
6	Walk (12 m)	Stair up (11 steps)	Walk (12 m)	Turn_3	Walk (12 m)	Stair down (11 steps)	Walk (12 m)	Paved	Paved
7	Run (12 m)	Stair up (11 steps)	Run (12 m)	Turn_3	Run (12 m)	Stair down (11 steps)	Run (12 m)	Paved	Paved

3. Algorithm design

We reasoned that the detection of strides may be preferred over the detection of steps to provide more robust results and more similar output across sensor positions. The developed algorithm is in essence a cross-correlation procedure, where, like conventional procedures, the distance between correlation peaks correspond with periodicity of the signal (step or stride cadence). However, with conventional methods spurious correlation peaks do occur, causing false positives in the step or stride detection. To reduce the number of false positives, the detected correlation peaks are subsequently verified using the Sylvester's criterion (SC). A peak is verified as a cycle (stride) when the accelerations in all directions of the preceding signal (part A) correlate positively with all directions in the incoming signal (part B). The algorithm as a whole is further referred to as the Cadence Detection Algorithm (CDA) and will be explained in greater detail in the next section.

3.1. Pre-processing

Fig. 1 describes the seven-step algorithm. The first three steps of the algorithm are required for pre-processing and to verify sensor movement. First acceleration data, initially a 4 s epoch, are buffered. The first 2 s (A) are correlated with the last 2 s (B) in the buffer. The duration of A remains 2 s during the process. The buffer length of B starts with 2 s and is adjusted in next iterations according to recent determined cycle durations (Fig. 1). Once the buffer contains sufficient data, the accelerometer data are pre-processed. The buffered tri-axial accelerations are resampled by linear interpolation to 50 Hz and smoothed with a 4th order median filter. The interpolation is done mainly to remove jitter (fluctuating sample rate), in view of later implementation on the smart-phone. In the fourth step of the algorithm, a compliant movement check is done to decide if the signal contains a potentially meaningful movement. The pre-processed signal is considered to contain a potentially meaningful movement when the square root of the summed variance of the pre-processed signal exceeds 0.5 m s^{-2} (Eq. (1)). Resampling and the movement check are useful to reduce the computational load. The threshold for the movement detection (0.5 m s^{-2}) was derived from the measured data in this study and found to be sufficiently sensitive to include all real events.

$$movement = \sqrt{var(B_x), +var(B_y) + var(B_z)} > 0.5\ \mathrm{m \cdot s^{-2}} \qquad (1)$$

3.2. Detection and validation

The fifth step of the algorithm is the most relevant step for understanding the benefit of the current algorithm, as it distinguishes this algorithm from previous correlation procedures by validating the correlation peaks. A mathematical description of these steps

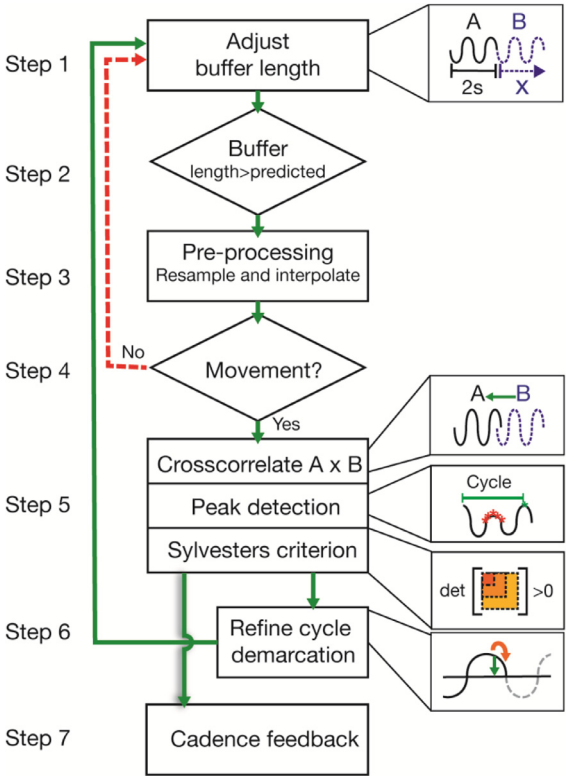

Fig. 1. Flowchart of the CDA. The process follows 7 steps: (1, 2) First two steps, tri-axial accelerations are determined and buffered. (3) During pre-processing jitter is removed and sample frequency is interpolated to 50 Hz. (4) Before further calculations are performed there is a compliant check to verify that there is sufficient amplitude to count as a movement. (5) Subsequently, the duration of the cycle is determined by verifying peaks with the Sylvester's criterion (SC). (6) For demarcation of the cycle boundaries, the algorithm 'snaps' to a nearby point with low summed acceleration. (7) Lastly, cadence is calculated from the result of the correlation spectrum.

can be found in Appendix A. When part B has a negative overlap of exactly one movement cycle (stride) a correlation peak is expected in the correlation spectrum. With validation of this peak, the algorithm can determine whether the peak indeed corresponds with one cycle. To this end, four sub-steps are applied: (a) All three directions in part A of the acceleration signal are cross-correlated with all three directions in part B, resulting in nine (3×3) correlation traces. (b) The correlation traces are summed and differentiated. Peaks are denoted by the change in sign from positive to negative. (c) The nine correlation traces at the selected peak index are 3rd-order averaged. (d) The SC is applied to verify each peak and two neighbouring samples. The SC is applied on M_i. M_i

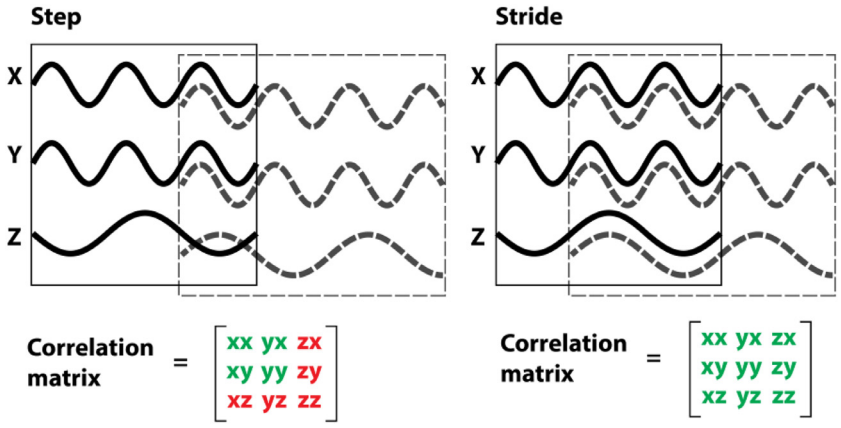

Fig. 2. Sylvester's Criterion verification for a step and stride. The figure illustrates the correlation procedure and the resulting correlation matrix summed with its transpose. The second signal slides back over the first signal. With the overlap of one step, this results in the left correlation matrix. With the overlap of one stride, the result is shown in the right correlation matrix. When the correlation matrix is positive definite (at the stride), the Sylvester's Criterion tests positive. This is the case when acceleration signals of all directions are positively correlated.

Table 2
Activity descriptive statistics (total, median, interquartile range (IQR)) for various activities and over all subjects.

Activities	Activities count		Stride count		Duration (s)		Speed (m s^{-1})
	Total	Median ± IQR	Total	Median ± IQR	Total	Median ± IQR	Median ± IQR
Walk[a]	204	11 ± 1	799	34 ± 14	1885	9.6 ± 5.5	1.5 ± 0.4
Run[a]	669	33 ± 7	5444	242 ± 80	4400	5.5 ± 5.2	3.4 ± 1.3
Sprint 1[a]	23	1 ± 0	347	15 ± 4	207	8.8 ± 2.9	5.7 ± 3.6
Sprint 2	21	1 ± 0	554	30 ± 7	357	17.1 ± 4.7	5.2 ± 1.9
Turn[a]	241	12 ± 2	1121	56 ± 30	881	3.0 ± 1.7	3.2 ± 2.0
Answer phone[a]	42	2 ± 0	556	26 ± 6	583	13.3 ± 4.0	2.0 ± 0.9
Slalom[a]	69	3 ± 0	508	25 ± 8	346	5.0 ± 1.3	3.3 ± 0.9
Speed ladder[a]	74	4 ± 0	318	16 ± 6	186	2.5 ± 0.9	3.6 ± 0.9
Stair_up[b]	70	4 ± 0	405	23 ± 2	334	4.2 ± 2.3	1.9 ± 1.2
Stair_down[b]	**70**	**4 ± 0**	**379**	**22 ± 2**	**285**	**4.1 ± 1.7**	**1.8 ± 0.9**

Sprint1: sudden start and stop. Sprint2: gradual speed increase/decrease.
[a] Activity was performed on pavement and grass.
[b] Activity was performed during walking and running.

is calculated by the correlation matrix at the peak, summed with its transpose (Eq. (2)). The SC states that the 3×3 matrix M_i is positive-definite if the determinants associated with all upper-left submatrices of M_i are positive (Eq. (3)). This indicates a positive correlation independent of sensor orientation (see Appendix A for details).

$$M_i = X_i^m + X_i^{m\mathrm{T}} \tag{2}$$

$$\mathrm{SC}_i = \det\left(M_{i,(1,1)}\right) > 0 \;\&\; \det\left(M_{i,(1,1),(1,2),(2,1),(2,2)}\right) > 0 \;\&\; \det(M_i) > 0 \tag{3}$$

3.3. Adjustment of the cycle demarcation

The sixth step of the algorithm is used to refine stride duration and demarcate cycle boundaries. Note that correlation peaks do not necessarily coincide with spatiotemporal events such as heel strike. Therefore, also small phase shifts between sequential strides may cause small errors in the determined stride duration. As a generic solution, the stride duration is corrected by snapping from the estimated cycle-end, to a point where acceleration is minimal. To this end, the accelerations are mean-centered and summed within the range of ±0.5 times the cycle duration (period) around point j (Eq. (4)). The positive to negative zero-crossing nearest to j is chosen as cycle-end. For ongoing movements, this point is used as the start of the next cycle, resulting in a recurring unspecified spatiotemporal moment within the cycle.

$$Acc_{xyz} = \sum_{i=j-0.5*period}^{j+0.5*period} \langle a_{x,i}\rangle + \langle a_{y,i}\rangle + \langle a_{z,i}\rangle \tag{4}$$

Where j is the index estimated by the period found in step 5.

3.4. Buffer length adjustment

Finally, the algorithm goes back to step 1, but buffer length is adjusted. A minimal buffer length reduces computational load and prevents feedback latency. The required length of the buffer is estimated from the previous cycles and depends on the presence of a cycle in the previous iteration. When a cycle has been found in the immediately preceding iteration, 1.5 times the average cycle length over the last 5 iterations is used to determine the next buffer length, where missing cycles are ignored. Note that the buffer length is slightly over-estimated to ensure inclusion of a full cycle in the next iteration. When the preceding iteration did not result in a positive outcome, the buffer length is estimated by multiplying the current buffer length by 1.2 to a maximum of 2 s. The scaling of 1.2 times the buffer length was determined empirically and the maximum of 2 s corresponds with 30 strides·min^{-1}, which is sufficiently long for any kind of walking and running. Note, that the buffer length is adjusted to the most recently found cycle durations, e.g. it will shorten in length when cadence is increasing and vice versa.

3.5. Cadence feedback

In the seventh step, cadence is calculated using Eq. (5) after which the signal is 5th-order median filtered. Where $(t_i - t_{i+1})$ denotes the difference in timestamps associated with the strides.

$$Cadence = 60/(t_i - t_{i+1}) \quad (5)$$

3.6. Reference signal

To evaluate the CDA, reference strides were found using a second, offline algorithm written to detect landing impacts from foot sensor data. For the reference algorithm, the gyroscope and data were low-pass Butterworth filtered (resp. 10 Hz, 5th order and 3 Hz, 1st order). Strides were detected by the zero-crossings from the filtered gyroscope data and preserved if they were accompanied by both an average gyroscope peak above $5^\circ\ s^{-1}$ and a square root summed squared acceleration peak above 12 m s^{-2}. Visual inspection of the accelerometer and gyroscope traces in combination with video footage was used to verify the reference strides and sporadic corrections were made manually where needed.

4. Analysis

First, the performance of the CDA was evaluated for the 10 sensor positions by comparison with the reference strides. To this end, both true positives (TP) and false positives (FP) were calculated. Second, the cadence feedback was compared with three conventional correlation procedures. The data were processed and analysed with (R2014b, MathWorks Inc., Natick, MA, USA).

4.1. Direct comparison with reference strides

The calculation of the TP's and the FP's was done as follows. First, the detected strides were paired with the reference strides based on minimal differences in timing. Matching pairs signify TP's, while detected strides lacking a reference counterpart signify FP's and the remaining reference strides represent false negatives (FN). For the various sensors, the timing of cycle demarcation is not expected to coincide exactly with reference strides measured at the foot. Therefore, the difference between TP's and the reference signal was first calculated; 3rd-order median filtered and subtracted from the timestamps of the strides detected by the algorithm. With the correction for a possible small (several ms) shift, the TP's were then re-calculated. The TP's and FP's were expressed as percentages of the total number of reference strides (resp. TPR and FPR). To take into account both the TP's and FP's, F1-scores were used (Eq. (6)) as calculated according to Bejarano et al. [6]. The F1 scores were used to compare the accuracy of the 10 sensor positions in a one-way ANOVA over the subject's. Games-Howel posthoc analysis was performed to determine significant main effects ($p < .05$).

$$Precision\ (P) = TP/(TP + FP) \quad (6)$$

$$Recall\ (R) = TP/(TP + FN)$$

$$F1_{score} = 2PR/(P + R)$$

4.2. Calculation of cadence feedback

The ultimate goal of the algorithm described is to provide cadence feedback. To evaluate the accuracy of CDA in this regard, the cadence signal (from step 7) was interpolated to a 3 Hz grid, to allow direct comparison with the reference cadence. A percentage feedback error was calculated using (Eq. (7)). An 80%-percentile error was calculated from this feedback error to express the range of the absolute error. A feedback score was calculated using the feedback error (Eq. (8)). These feedback scores were obtained from calculations over the complete circuit including the disturbances due to gait-related activities.

$$\text{Feedbackerror}(i) = \left(\frac{|Ref\ cadence(i) - Algorithm\ cadence(i)|}{ref\ cadence(i)} \right) \times 100\% \quad (7)$$

$$\text{Feedback score}(i) = 100\% - \text{Feedback error}(i) \quad (8)$$

where i is the index in the interpolated cadence trace.

4.3. Comparison with conventional correlation procedures

The CDA differs from the conventional correlation procedures by the additional validation of the correlation peak using the SC (Fig. 1, Step 5). Therefore, to assess the added value of the SC for the provision of instantaneous feedback, step five of the algorithm was replaced by each of the three conventional correlation procedures. These three procedures were: unbiased cross-correlation (b), unbiased autocorrelation (c) and biased autocorrelation (d). The step durations for the cross-correlation and unbiased autocorrelation (Fig. 3b, c) were calculated as the time to the first peak in the correlation spectrum. For the biased autocorrelation, the time to the highest peak in the correlation spectrum was used as step duration (Fig. 3d). For these procedures, the magnitude of acceleration was used in the correlation procedure to deal with the unknown sensor direction (Fig. 3b, c, d). Because magnitude is used, the procedures cannot differentiate between steps or strides and are therefore implemented as step-detection procedures. This implies that the limits of the stride duration (0.4–2 s) were set to 0.2–1 s for the step duration and the (stride based) cadence feedback was doubled.

5. Results

5.1. Direct comparison with the reference strides

In total 14,881 strides were evaluated (mean ± SD: 676 ± 92.7 per subject) (see Table 2 for the details of each activity). For the seven dedicated sensors and the three smartphones, mean true positive rates (TPR) ranged from 85.6 to 100.0% and false positive rates (FPR) from 0.0 to 2.9% during walking, running, and both types of sprinting (Fig. 2). The mean score over the all circuits, including all disturbances and transitions, ranged, for TPR from 72.9 to 91.2%, and for FPR from 0.1 to 3.4% (Fig. 4). Using one-way ANOVA, significant differences were found in F1-scores between sensor positions (Welch's $F\ (9,\ 81.07) = 12.35,\ p < .001$). Post-hoc analyses indicated that the accuracy was significantly lower for the hand-held sensor (mean ± SD: 82.94 ± 6.03%) compared to all other sensor positions ($p < .001$).

5.2. Comparison between sensor positions

The feedback score was used to calculate a median agreement over the subjects. For the CDA, these ranged from 98.8% (Hand) to 99.0% (Heel) for walking, running and the two sprinting conditions. The 80%-percentile feedback error ranged from 2.5% (Instep) to 3.2% (Hand), indicating that for 80% of the detected strides feedback errors fell within this range. For the complete circuit including all interruptions, median agreement ranged from 98.6 to 98.9% and 80%-percentile feedback error from 3.1 (Heel) to 4.6% (Hand).

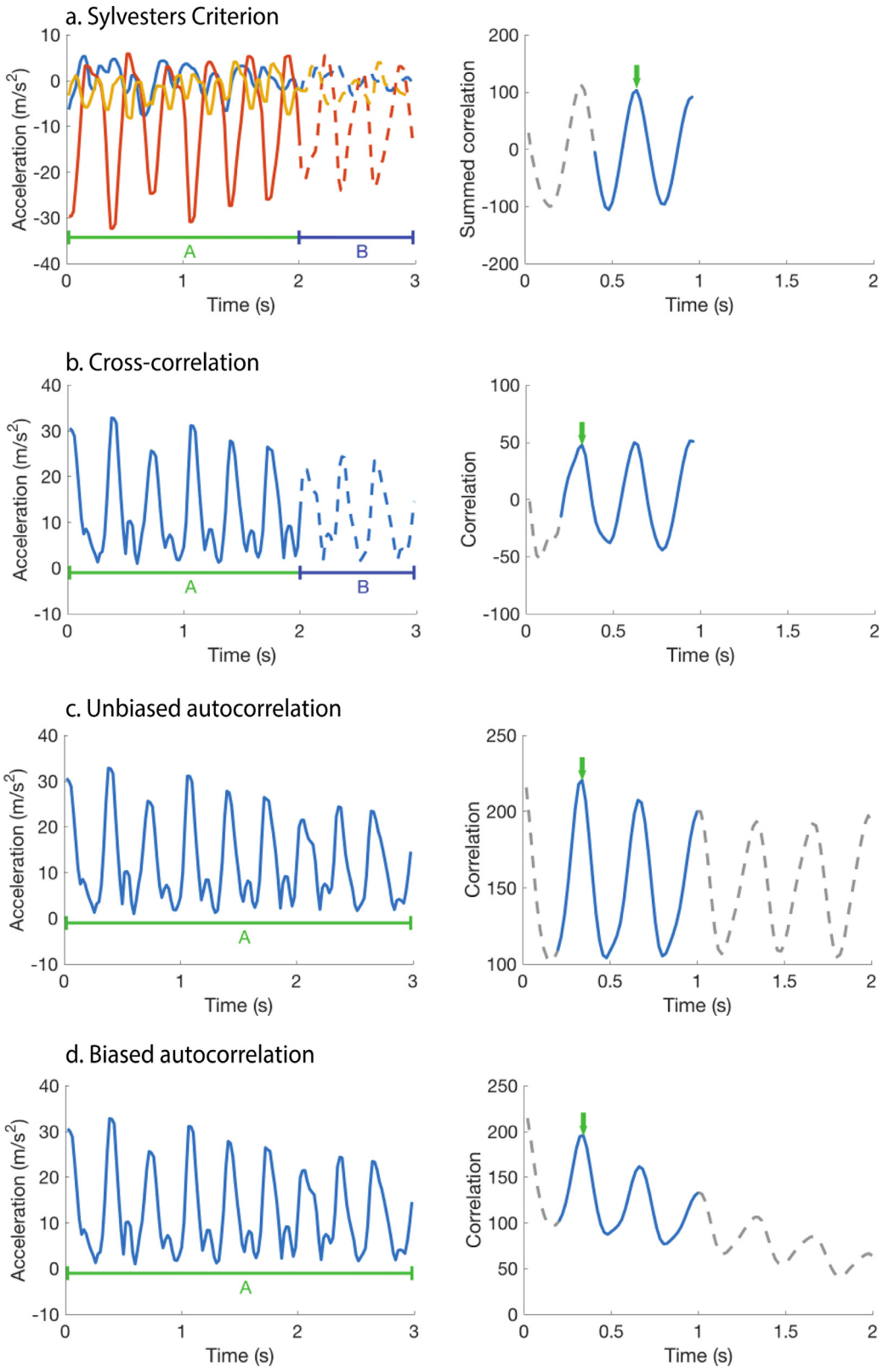

Fig. 3. Correlation procedures. The respective procedures are based on: (a) The Sylvester's criterion (SC), as used in the CDA; (b) Cross-correlation; (c) Unbiased autocorrelation; (d) Biased autocorrelation. The left panels display the signals used as input for the correlation. Only the SC (a) is reliant on separate tri-axial accelerations. The other procedures use magnitude accelerations as input for the correlation procedure. The cross-correlation based procedures (a, b) use signals divided into sequential parts A and B, where the correlation signal will be as long as the duration of B. Instead, the autocorrelation-based procedures (c, d) use a replica of the whole signal. The right panels display the signal used for peak detection. The right panel of the SC displays the sum of the 3×3 correlation signals resulting from tri-axial signal. For the other procedures, the correlation output is used. The dotted line is the part of the signal that can be ignored since these peaks fall outside the window in which the next stride or step can be expected. Only the SC (a) procedure is a stride detection procedure, while the other procedures can be classified as step-detection procedures and window limits are thus set accordingly (resp. 0.4–2 s and 0.2–1 s).

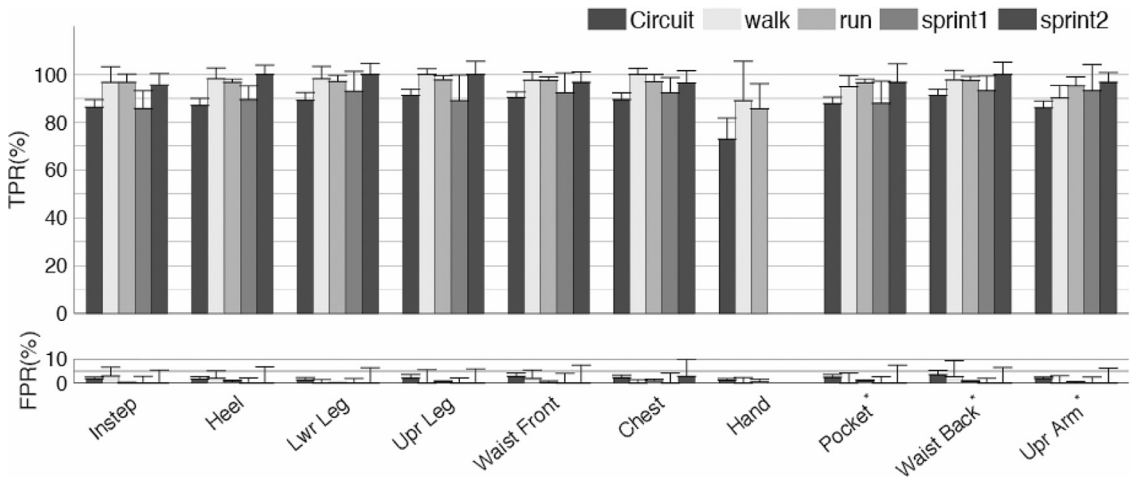

Fig. 4. True and false positives rates. The bars represent the true (upper: TPR) and false positives rates (lower: FPR) detected by the CDA. The rates are based on all sensor positions for the complete circuit, for walking, running and sprinting with a sudden start-stop (sprint1) and sprinting with a gradual speed increase-decrease (sprint2). Note the small number of false positives detected by the CDA in all conditions. The asterisk (right most three conditions) denotes the smartphone measurements.

5.3. Comparison between correlation procedures

Fig. 5 illustrates the median feedback scores for the various sensor positions between the four correlation procedures. The SC-based procedure provides substantially higher cadence feedback agreement (mean ± SD: 98.9 ± 0.2%) relative to the three other correlation procedures: cross-correlation (87.3 ± 13.5%), biased autocorrelation (73.0 ± 16.2) and unbiased autocorrelation (82.2 ± 20.6). Note that both the between sensor variation and the between subject variation are very low for the SC-based procedure (Fig. 5a).

6. Discussion

Correlation procedures are commonly used to determine the fundamental movement frequency from acceleration patterns. Conventional correlation procedures depend on sensor position and orientation and are prone to false negatives or positives. The CDA described in this paper is robust to variation in sensor placement and the validation of the correlation peaks improved accuracy compared to conventional correlation procedures. More specifically, the CDA excelled especially in a low number of FP's, which is imperative for an accurate estimation of cadence.

6.1. Comparison between procedures for cadence feedback

Whilst the CDA performance is completely independent from sensor placement, the cross-correlation (Fig. 5b) and the unbiased autocorrelation (Fig. 5c) only provided reasonably well results for sensors placed at central positions, e.g. the waist or chest, although they also performed reasonable for the upper-arm, a commonly used developed with the limitations position for carrying smartphones. The biased autocorrelation (Fig. 5d) procedure was less accurate for all sensor positions. Depending on the sensor position, algorithms may predominantly be more sensitive to steps or strides. The underlying assumption is that either the step or stride frequency consistently dominates the correlation spectrum. Our results show that this assumption is not valid under many conditions as the conventional procedures seem to alternate between detection of steps and strides or wrongly detect other spurious correlation peaks. Overall, the conventional correlation procedures find more false positives and as our results show, even in positions where one would expect more consistent findings for detected strides (instep, heel). The new SC-based procedure is independent of sensor position, It showed high robustness between participants with differences in running style, sensor fixation and speeds. It performed well across activities including short gait interruptions and a wide speed range and generated robust results across all sensor positions. This illustrates that it was not affected by sensor alignment, fixation or orientation. Note that, despite the deliberately introduced highly variable measurement conditions, the CDA did not require any calibration or parameter adjustments. Outside laboratory settings, users wear sensors as they prefer, which leads to a wide variety of possible sensor positions, orientations and fixations. Therefore, the high adaptability shown by the CDA is an important improvement.

6.2. Real-time processing and adaptability

Only a few of the algorithms in the literature were designed for real-time detection of stride times [4,6,22] or have been tested using smartphone data [15,17]. The correlation procedure was chosen as a basis for the CDA because of its known low computational load and because it does not rely on thresholds. The computational load is further minimized by estimating required buffer length, pre-terminating the process when possible and direct stride-to-stride comparison with cross-correlation. The SC can in principle be applied to all correlation methods, but cross-correlation on strides is preferred to make the algorithm adapt quickly, prevent feedback latency and to improve accuracy.

6.3. Ecological validity

Most often, algorithms are not designed to deal with the challenges of everyday conditions, or they are not tested in a representative manner. Everyday conditions involve diverse short gait episodes, often with sudden transitions. In contrast, most published algorithms have been tested within constrained conditions. For example, during steady-state walking only, sometimes even while walking in sync with a metronome [6,17], or for a small number of steps only. While other algorithms require multiple sensors or a specific sensor orientation. An additional limitation of many studies is that algorithms are validated using averages over time-intervals [2]. With the use of averages, FP's and FN's could cancel each other out. For example, Fortune et al. [2] did test their algorithm on jogging, reporting 97% (IQR: 6%) median agreement, but used average stride counts instead of instantaneous comparisons and only over circuits of 8.5 m. In addition, their algorithm required input from three given sensors with a known orientation.

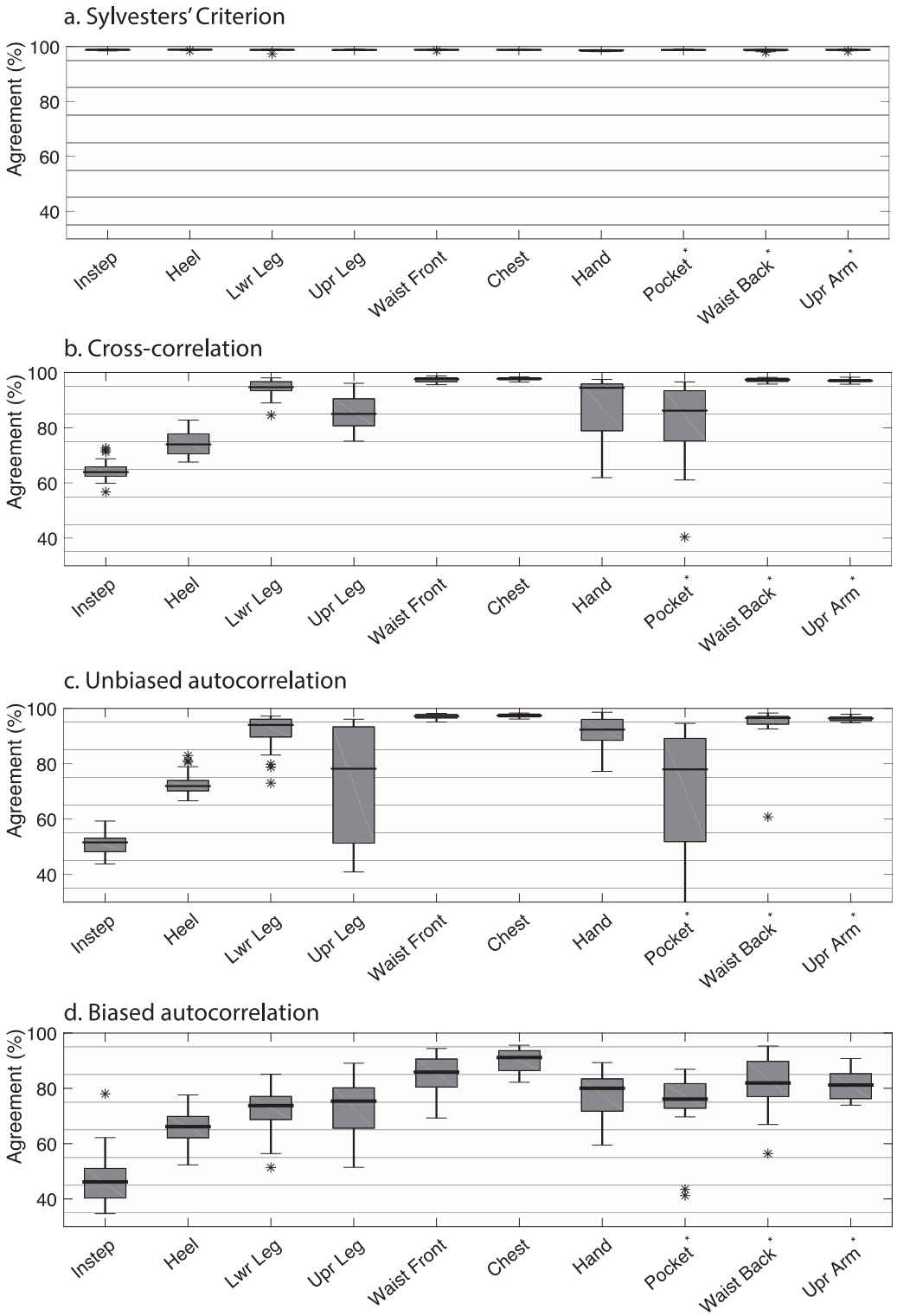

Fig. 5. Cadence feedback scores. Boxplot of results regarding the cadence feedback on the complete circuits, including the different gaits, activities and transitions, respectively for the Sylvester's criterion (SC) (a), the Cross-correlation (b), Unbiased autocorrelation (c) and the Biased autocorrelation (d) based procedures. For this comparison, the durations of either strides (a) or steps (b–d) found by the each procedure was 5th order median filtered and interpolated to a 3 Hz grid to allow instantaneous comparisons (see Material and procedures for details) on the percentage agreement. Note the high percentage agreement (> 97%) as well as the very small ranges between subjects and sensor positions for the SC (a) compared to the other algorithms.

Therefore, in the present study, the timing of reference strides with the algorithm was tested instantaneously. In addition, we used a wide speed range (1.5–5.7 m s^{-1}) and validated across a diversity of signals derived from 10 different sensor positions. To our knowledge, there has not been an algorithm that was tested this rigorously, while dealing with all challenges (orientation, position, gait-activities) simultaneously. Noteworthy is that the smartphones, despite their weight and the possible negative influence of lower sample frequencies and jitter, did not differ in performance from the dedicated (small, light-weight) sensors. This further illustrates

the high ecological validity of our study compared to the existing literature.

6.4. Limitations

In this study, we compared the algorithm with correlation procedures, since the algorithm can be regarded as an extension to conventional correlation procedures. By plugging in these algorithms, we were able to make a direct comparison, since the same pre-processing could be used. However, the performance of these procedures may be improved by other filters or window-lengths or additional thresholds. For example, the autocorrelation procedures can be improved by increasing window-length. With the disadvantage that this would delay the feedback, but also reduce accuracy of the immediate frequency estimate, since autocorrelation procedures provide an average over the selected window length. Especially during irregular or varying patterns such as during speed changes or pathological gait, longer window lengths would lead to errors. For the CDA, the effective window length does not need to be larger than one stride to provide accurate results. It remains to be investigated how it will compare to other algorithms in challenging situations. The CDA was developed with the limitations of smartphone processing in mind. Moreover, during the development we have implemented the algorithm successfully on the smartphones. However, the performance in terms of computational load has not yet been tested extensively and further optimizations might be required to decrease computational load. The CDA was not designed to detect specific spatiotemporal gait events, since a generic solution for specific event-detection that works across all sensor positions is most likely elusive. However, for specific applications, it could be interesting to expand the algorithm with the calculations of specific spatiotemporal events. The low number of FP's will allows calculations of contact time [25,26], vertical oscillation [27] and arm swing [28].

6.5. Population

The algorithm was specifically designed for the use of walking and running during sport activities. For this reason, the algorithm was only tested with young subjects. The large variation between sensor signals, as a consequence of variation in positions, fixations and gait types, may well outweigh any potential bias caused by the limited age-range of our subjects. However, slow movements with low amplitude that may occur with aging could lead to a decrease in performance of the CDA. In general, we would expect diminished performance in situations with low signal-to-noise ratio and/or when stride-to-stride variation is high. Therefore, for specific patient groups (e.g. Parkinson patients) the CDA may face additional challenges and performance in such specific situations remains to be investigated.

6.6. Application and future research

Pathological gait is often asymmetrical and sensors seldom are perfectly aligned centrally on the body. Under these conditions accurate detection of strides is a challenge. We expect that our CDA will also perform well under such circumstances. Technically, the CDA detects competed cycles. Therefore, we would expect the CDA to perform also well during other cyclic activities. This would make the algorithm suitable for multi-sport purposes. In future research, the performance of the CDA could be evaluated during other cyclic activities (e.g. swimming, cycling, rowing, skating) and for patient populations with irregular gait patterns. In addition, complimentary algorithms could be developed to add automatic activity recognition (e.g. walking, running or cycling), or to detect specific spatiotemporal events (e.g. initial foot contact or toe-off).

7. Conclusion

The proposed algorithm (CDA) proved to be consistently more accurate in detecting cadence compared to conventional correlation procedures, across gaits, subjects and sensor positions. By validating completed cycles (strides) the CDA overcomes the limitation of sensor position accuracy of conventional correlation procedures. The CDA was designed to be suitable for real-time smartphone-processing and was challenged by including a diversity of gait-related activities to ensure its robustness in everyday conditions. These results encourage exploring the CDA in other cyclic sports like cycling, rowing, cross-country skiing, speed skating and other challenging situations such as analysis of patients' gait.

Conflict of interest

The authors state that there were no financial or other relationships that may represent any conflict of interest.

Ethical approval

The study was approved by the local ethics committee of the Vrije Universiteit Amsterdam. All subjects provided written consent to the collection and use of data reported in the manuscript.

Acknowledgments

This study was partially supported by a grant from COMMIT project P3, titled "Sensor-based engagement for improved health". The funding agency played no role in the design of the study or the interpretation of the results. The algorithm was simultaneously developed to work on a smartphone. We thank S. Neacsu for translating the Matlab code and optimizing the Java code for the smartphone application.

Appendix A

In the next section, the validation of correlation peaks using the Sylvester's Criterion (SC) will be explained in more detail. Cross-correlation of sequential strides produces correlation peaks in the correlation spectrum at the overlap of one step or one stride. Depending on the sensor position (on a limb or on the trunk) either steps or strides may dominate the correlation spectrum. In addition, there may be additional spurious correlation peaks. When this happens inconsistently, the estimated frequency result will become unreliable. The SC is used to validate the peaks in the correlation spectrum to consistently denote only the peaks that correspond with strides, or more generally, cycles.

In human gait, with the sensor perfectly aligned with the Earth and anatomical axes and centrally placed on the body, the dominant frequencies of the three axes of acceleration differ. The frequencies of the vertical and horizontal will be twice the frequency measured in the mediolateral axis. Consequently, when we have two sequential strides, the cross-correlation at one step overlap between axes will be negative for the mediolateral direction, while it will be positive in the vertical and horizontal direction (Fig. 2 on the left). At one stride overlap, all the directions will provide positive correlations (Fig. 2 on the right). When the sensor is not perfectly aligned with the Earth and anatomical axes the amplitude of the mediolateral signal is blended with the traces of the other two axes. Consequently, the negative correlation of the mediolateral axis at one step overlap may be unobserved, while the power of the correlation will be reduced. Therefore, it is better to verify that the correlation is positive for any direction, rather than isolating or combining accelerations from 3 sensor axes. This is done by using the correlations between all axes instead, thus the

whole correlation matrix (Eq. (A.1)), and verifying that this matrix is positive-definite, rather than only verifying that it has positive values on the diagonal.

The procedure starts with calculating the cross-correlation as:

$$\boldsymbol{X_i} = [\boldsymbol{A_i}] \times [\boldsymbol{B_i}]$$
$$\boldsymbol{X_i} = \begin{bmatrix} A_xB_x & A_yB_x & A_zB_x \\ A_xB_y & A_yB_y & A_zB_y \\ A_xB_z & A_yB_x & A_zB_z \end{bmatrix} \quad \text{(A.1)}$$

where $\boldsymbol{A_i}$ is a $i \times 3$ matrix of the last i samples of signal A and $\boldsymbol{B_i}$ is the $i \times 3$ matrix of the first i samples of signal B. $\boldsymbol{X_i}$ is the cross-correlation matrix (with 3×3 correlation traces) with an overlap of length i. Then, correlations are summed:

$$\boldsymbol{X_{sum,i}} = \boldsymbol{X_{i,(1,1)}} + \boldsymbol{X_{i,(2,2)}} + \boldsymbol{X_{i,(3,3)}} \quad \text{(A.2)}$$

From $\boldsymbol{X_{sum,i}}$ the indices of the peaks ($\boldsymbol{i_{peak}}$) are selected by finding the index where $\boldsymbol{diff}(\boldsymbol{X_{sum,i}})$ changes direction from positive to negative. The sum is here more preferable than the often-used root mean square, as it leaves the sign of the amplitudes as it is.

At each peak index and adjacent samples the Sylvester's Criterion (Eqs. (A.4)–(A.5)) is tested. Adjacent samples are tested in a specific order $\boldsymbol{i_{peak}} + [-1\ +1\ -2\ +2]$.

$$\boldsymbol{X_i^m} = \frac{1}{3}\sum_{\boldsymbol{j}=-1}^{1} \boldsymbol{X_{i+j}} \quad \text{(A.3)}$$

Where $\boldsymbol{X_i^m}$ is the 3rd-order averaged correlation matrix at index $\boldsymbol{i}$. In this study, the selected indexes were 3rd-order averaged (the signals' frequency was forced to 50 Hz in a previous step) for more robust results.

The Sylvester's Criterion is defined by Eqs. (A.4) and (A.5).

$$M_i = X_i^m + X_i^{m\mathrm{T}} \quad \text{(A.4)}$$

$\boldsymbol{M_i}$ is calculated for the nine cross-correlation coefficients at the peak index by summing ($\boldsymbol{X_i^m}$) with its transpose ($\boldsymbol{X_i^{m\mathrm{T}}}$). This operation results in a symmetrical matrix ($\boldsymbol{M_i}$).

$$\boldsymbol{SC_i} = \mathbf{det}\left(\boldsymbol{M_{i,(1,1)}}\right) > 0\ \&\ \det\left(\boldsymbol{M_{i,(1,1),(1,2),(2,1),(2,2)}}\right) > 0\ \&\ \mathbf{det}(\boldsymbol{M_i}) > 0 \quad \text{(A.5)}$$

The SC verifies the 3×3 matrix $\boldsymbol{M_i}$ as positive-definite when the determinants of all square upper left corner sub-matrices of M are positive (Eq. (A.5)). This indicates a positive correlation independent of sensor orientation.

Suggested readings

Weisstein, Eric W. "Positive Definite Matrix." From MathWorld–A Wolfram Web Resource. http://mathworld.wolfram.com/PositiveDefiniteMatrix.html.

References

[1] Foster RC, Lanningham-Foster LM, Manohar C, McCrady SK, Nysse LJ, Kaufman KR, et al. Precision and accuracy of an ankle-worn accelerometer-based pedometer in step counting and energy expenditure. Prev Med (Baltimore) 2005;41:778–83. doi:10.1016/j.ypmed.2005.07.006.

[2] Fortune E, Lugade V, Morrow M, Kaufman K. Validity of using tri-axial accelerometers to measure human movement – part II: step counts at a wide range of gait velocities. Med Eng Phys 2014;36:659–69. doi:10.1016/j.medengphy.2014.02.006.

[3] Guiry JJ, van de Ven P, Nelson J, Warmerdam L, Riper H. Activity recognition with smartphone support. Med Eng Phys 2014;36:670–5. doi:10.1016/j.medengphy.2014.02.009.

[4] Hanlon M, Anderson R. Real-time gait event detection using wearable sensors. Gait Posture 2009;30:523–7. doi:10.1016/j.gaitpost.2009.07.128.

[5] Alvarez JC, Alvarez D, López A, González RC. Pedestrian navigation based on a waist-worn inertial sensor. Sensors 2012;12:10536–49. doi:10.3390/s120810536.

[6] Chia Bejarano N, Ambrosini E, Pedrocchi A, Ferrigno G, Monticone M, Ferrante S. A novel adaptive, real-time algorithm to detect gait events from wearable sensors. IEEE Trans Neural Syst Rehabil Eng 2014:4320. doi:10.1109/TNSRE.2014.2337914.

[7] González RC, López AM, Rodriguez-Uría J, Álvarez D, Alvarez JC. Real-time gait event detection for normal subjects from lower trunk accelerations. Gait Posture 2010;31:322–5. doi:10.1016/j.gaitpost.2009.11.014.

[8] Hundza SR, Hook WR, Member L, Harris CR, Mahajan S V, Leslie PA, et al. Accurate and reliable gait cycle detection in Parkinson's disease. IEEE Trans Biomed Eng Transitions Neural Syst Rehabil Eng 2014;22:127–37.

[9] Palayo P, Alberty M, Sidney M, Potdevin F, Dekerle J. Aerobic potential, stroke parameters, and coordination in swimming front-crawl performance. Int J Sports Physiol Perform 2007;2:347–59.

[10] van Ingen Schenau GJ, de Groot G, de Boer RW. The control of speed in elite female speed skaters. J Biomech 1985;18:91–6. doi:10.1016/0021-9290(85)90002-8.

[11] Hofmijster MJ, Landman EHJ, Smith RM, Van Soest a JK. Effect of stroke rate on the distribution of net mechanical power in rowing. J Sports Sci 2007;25:403–11. doi:10.1080/02640410600718046.

[12] de Ruiter CJ, Verdijk PWL, Werker W, Zuidema MJ, de Haan A. Stride frequency in relation to oxygen consumption in experienced and novice runners. Eur J Sport Sci 2013:37–41. doi:10.1080/17461391.2013.783627.

[13] Hobara H, Sato T, Sakaguchi M, Nakazawa K. Step frequency and lower extremity loading during running. Int J Sports Med 2012;33:310–13. doi:10.1055/s-0031-1291232.

[14] Mosa ASM, Yoo I, Sheets L. A systematic review of healthcare applications for smartphones. BMC Med Inform Decis Mak [Internet] 2012;12(1):1.

[15] Brajdic A, Harle R. Walk detection and step counting on unconstrained smartphones. In: UbiComp '13; 2013. p. 225–34.

[16] Ying H, Silex C, Schnitzer A, Leonhardt S, Schiek M. Automatic step detection in the accelerometer signal. In: 4th international work of wearable implant body sensor networks (BSN 2007), 13; 2007. p. 1–6. doi:10.1007/978-3-540-70994-7_14.

[17] Tarashansky A, Vathsangam H, Sukhatme GS. A study of position independent algorithms for phone-based gait frequency detection. IEEE Eng Med Biol Soc 2014:5984–7. doi:10.1109/EMBC.2014.6944992.

[18] Lester J, Hartung C, Pina L, Libby R, Borriello G, Duncan G. Validated caloric expenditure estimation using a single body-worn sensor. In: Ubicomp '09; 2009. p. 225. doi:10.1145/1620545.1620579.

[19] Moens B. Sensor evaluation for real-time pace and step detection for sonic interaction. COST/SID Reports 2010:1–12.

[20] Lewis JP Industrial L& M. Fast normalized cross-correlation. Vis Interface 1995;1995:1–7. doi:10.1007/s00034-009-9130-7.

[21] Aminian K, Najafi B, Büla C, Leyvraz PF, Robert P. Spatio-temporal parameters of gait measured by an ambulatory system using miniature gyroscopes. J Biomech 2002;35:689–99. doi:10.1016/S0021-9290(02)00008-8.

[22] Yang C-C, Hsu Y-L, Shih K-S, Lu J-M. Real-time gait cycle parameter recognition using a wearable accelerometry system. Sensors (Basel) 2011;11:7314–26. doi:10.3390/s110807314.

[23] Marschollek M, Goevercin M, Wolf K-H, Song B, Gietzelt M, Haux R, et al. A performance comparison of accelerometry-based step detection algorithms on a large, non-laboratory sample of healthy and mobility-impaired persons. Conf Proc IEEE Eng Med Biol Soc 2008;2008:1319–22. doi:10.1109/IEMBS.2008.4649407.

[24] Kim JW, Jang HJ, Hwang D-H, Park C. A step, stride and heading determination for the pedestrian navigation system. J Glob Position Syst 2004;3:273–9. doi:10.5081/jgps.3.1.273.

[25] Chapman RF, Laymon AS, Wilhite DP, McKenzie JM, Tanner DA, Stager JM. Ground contact time as an indicator of metabolic cost in elite distance runners. Med Sci Sports Exerc 2012;44:917–25. doi:10.1249/MSS.0b013e3182400520.

[26] Smith L, Preece S, Mason D, Bramah C. A comparison of kinematic algorithms to estimate gait events during overground running. Gait Posture 2015;41:39–43. doi:10.1016/j.gaitpost.2014.08.009.

[27] Saunders P, Pyne D, Telford R, Hawley J. Factors affecting running economy in trained distance runners. Sport Med 2004;34:465–85.

[28] Strohrmann C, Seiter J, Llorca Y, Tröster G. Can smartphones help with running technique? Procedia Comput Sci 2013;19:902–7. doi:10.1016/j.procs.2013.06.123.